19th Australasian Tunnelling Conference – Acosta-Martínez, Stewart and Hudson-Smith (Eds.)


# Modelling the impact of blasting on excavation perimeters

P.C. Dare-Bryan and E. Dixon
*Orica, Australia*

ABSTRACT: In hard rock civil projects blasting is often the preferred option for effective production rates in geometries and rock mass where mechanical excavation is less effective. However, blasting can result in increased damage into the excavation perimeters compared to mechanical excavation techniques. Understanding the impact of blasting within a particular environment is important for the long-term success of a project.

A large civil project in NSW, Australia, was experiencing variability in the conformance of tunnel perimeters after blasting and wanted an improved understanding of the impact of blasting on damage accumulating in the perimeters. Numerical simulations were conducted using a hybrid finite/discrete element program coupled with a non-ideal detonation model. The modelling included a detailed representation of the rock mass including pre-existing jointing and the in-situ stress state. The models assessed the impact of helper and perimeter holes on damage, highlighting the local variation caused by the interaction between explosive energy and jointing.

A subsequent study for a critical cavern excavation within the project assessed the impact of two perimeter designs; smooth wall blasting, which involves charging alternate holes with perimeter bulk product, and close-spaced line drilling of uncharged holes. The modelling indicates that smooth wall design produces greater damage close to the perimeter. However, at distances greater than 0.2 m into the perimeter, there is no significant difference between the two designs in the amount of damage accumulated in the rock mass.

## 1 INTRODUCTION

In civil tunnelling and cavern excavation removal of the rock mass can be done mechanically or by blasting. Mechanical can be preferred as it does not result in undulations of the perimeter that drill and blast require, allowing the mechanical means to excavate more accurately to the design perimeter. Additionally, mechanical methods limit potential damage accumulated in the rock mass at the perimeter. However, in many hard rock excavations the cost and slow progress rate of mechanical excavation means it is not a viable option for the project. Blasting has been demonstrated time and again to be an effective means of developing a wide range of underground excavations, sometimes in environmentally sensitive areas to very stringent design requirements. However, the success of the technique is highly dependent on an appropriate blast design being carefully applied with the appropriate consideration of the surrounding rock mass and any changes to the rock mass.

A highly complex large scale civil project in NSW, Australia was advancing tunnels in opposite directions and a range of varying rock masses. Inevitably this led to changes in the conformance of the post-blast perimeters. Numerical modelling was conducted to determine the impact of blasting in the least favourable direction with respect to the rock mass structure.

Further modelling work investigated the impact of two different perimeter designs on tunnels leading to a large cavern where the preferred perimeter design will be utilised to excavate the cavern.

## 2 BLAST MODELLING

The Mechanistic Blasting Model (MBM) is based on Elfen, a large dynamic finite/discrete element code (Owen et al., 1992). MBM simulates the non-ideal explosive loading of the blasthole wall and the subsequent fracturing and bulk motion of the surrounding rock mass due to stress/strain effects and the influence of dynamic gas loading in the blasthole and throughout the fracture network (Minchinton and Lynch, 1996, Dare-Bryan et al., 2012). Fracturing is handled by a strain-rate-dependent softening tensile failure Rankine plasticity model. Under sufficient fracturing, discrete elements are formed as separate, distinct polygonal elements made up of one or more finite elements; as such these discrete elements are fully deformable and can support stress and strain. The detonation of the explosives in the blasthole is modelled using data from a non-ideal detonation model (Kirby et al. 2014) to derive the influence of the rock confinement and blasthole diameter on the resulting velocity of detonation (VoD) and blasthole wall pressure-time profile. The post Chapman-Jouguet (CJ) pressure loading of the rock mass is handled dynamically by a gas flow model.

MBM is limited to two-dimensional geometries and can be run in two configurations:

- Plan view, where a section is taken perpendicular to the axes of the blastholes, to evaluate the interaction of multiple blastholes.
- Axisymmetric, where a section is taken through a single blasthole with the line of symmetry on the axis of the blasthole.

In this study, axisymmetric geometries were built taking a vertical section within the roof, in line with a helper hole and a perimeter hole to determine their impact on the rock mass. While plan view geometries were used to assess the impact of the charged and uncharged holes in smooth wall and line drilling design methodologies.

## 3 ROCK PROPERTIES

High-fidelity numerical models such as MBM require detailed information on the rock mass. Each rock domain requires data on the:

- Elastic properties: density, P-wave velocity, S-wave velocity, Young's Modulus and Poisson's ratio - these are associated with elastic stress wave propagation through the rock mass.
- Plastic properties: tensile strength, fracture energy - associated with fracture generation and propagation.
- Structural properties: major joint sets and discontinuities (dip angle, dip direction, spacing and persistence) - describes the in-situ rock structure.

The two rock types in this study are defined by the ratios of siltstone and sandstone, where a higher proportion of sandstone produces a more competent rock mass (Table 1). The fracture energy is a required input for the model failure criteria and is calculated from the fracture toughness tensile stress intensity factor ($K_{ic}$) which is not a parameter that is typically available from operations and so is often derived from literature. The major pre-existing structures within the rock domains are listed in Table 2.

Table 1. Elastic / plastic rock properties.

| Rock type | Siltstone / Sandstone | Sandstone / Siltstone |
|---|---|---|
| Density (g/cc) | 2.75 | 2.75 |
| Young's Modulus (GPa) | 48 | 58 |
| Poisson's Ratio | 0.25 | 0.25 |
| P-wave velocity (m/s) | 4577 | 5031 |
| S-wave velocity | 3411 | 2905 |
| Unconfined Compressive Strength (MPa) | 58 | 98 |
| Tensile Strength (MPa) | 8 | 11 |

| | | |
|---|---|---|
| Fracture Energy (N/m) | 100 | 100 |
| Fracture Toughness $K_{ic}$ (MPa.m$^{1/2}$)* | 2.0 | 2.25 |

*Derived from literature (Backers, 2005).

Table 2. Rock mass discontinuity data.

| Structure | Bedding Plane | Joint Set 1 | Joint Set 2 |
|---|---|---|---|
| Dip (°) | 30 | 80 | 80 |
| Dip Direction (°) | 050 | 210 | 130 |
| Nominal Spacing (m) | 0.3 | 0.3 | 1.0 |
| Nominal Persistence (m) | 5 | 2 | 5 |

## 4 PERIMETER DAMAGE MODELING

A typical blast design is shown in Figure 1, with the charging for the helper and perimeter holes displayed. All the blastholes are 45 mm in diameter and 3.2 m long. The helper holes are charged with a 0.8 g/cc straight emulsion bulk explosive, Subtek™. The bulk Subtek™ Control in the perimeter holes is a special formulation that is charged at an in-hole density of 0.6 g/cc, essentially over-gassed, the product does not sustain this density during the blast, and collapses down to a density of approximately 0.8 g/cc, this makes the charge partially decoupled from the hole. The air gap reduces the pressure applied to the hole wall, and reduces the confinement of the charge resulting in a lower VoD (and detonation pressures) compared to a fully coupled charge at 0.8 g/cc.

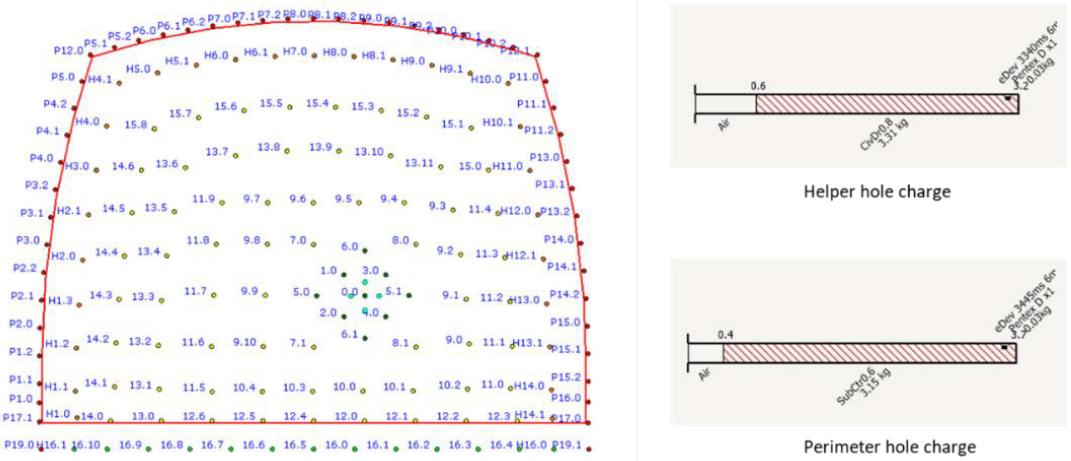


Figure 1. Typical design showing charging for the helper and perimeter holes.

### 4.1 *Perimeter model geometries*

Separate axisymmetric model geometries were created for a helper and a perimeter hole (Figure 2). The tunnel advance was in a southerly direction which results in the bedding plane (Table 2) cutting through the roof of the tunnel at an unfavourable angle. The helper hole geometry has the hole offset 0.8 m from the tunnel roof. The tunnels are at an approximate depth of 680 m and have in-situ stress conditions with a principal horizontal stress of approximately 30 MPa aligned north-south and a vertical stress of approximately 20 MPa. The red lines in geometries highlight the charged portion of the holes.

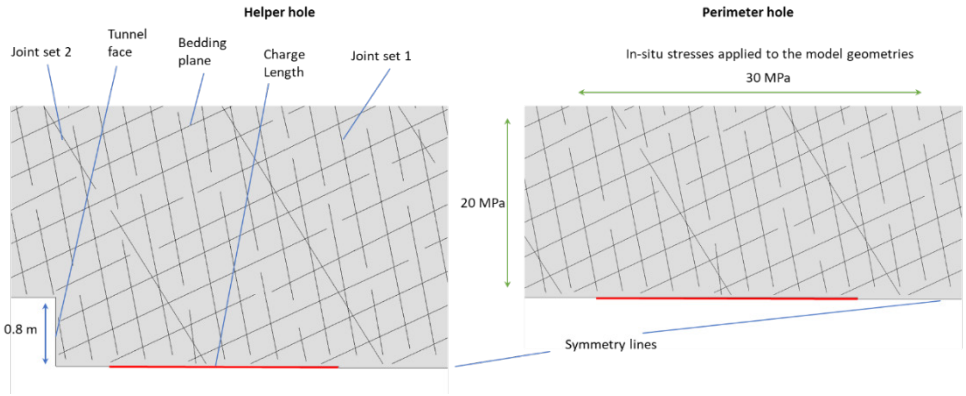


Figure 2. Model geometries for the helper hole (left) and the perimeter hole (right) showing the structures applied as discrete fracture networks and the in-situ stresses.

### 4.2 *Perimeter in siltstone/sandstone*

The plots of waveform velocity in Figure 3 are captured 0.5 ms after the charges have initiated and highlight the complex wave interaction with the structure in the rock mass, producing local variations in wave amplitude. The broken line through the plots 0.5 m above the perimeter is provided as a reference line. The plots of resulting damage (Figure 4) show minimal damage from the helper hole into the rock mass above the roof line and only limited damage from the perimeter hole into the rock mass above the roof line. The damage from the perimeter hole accumulates principally along the bedding plane discontinuity.

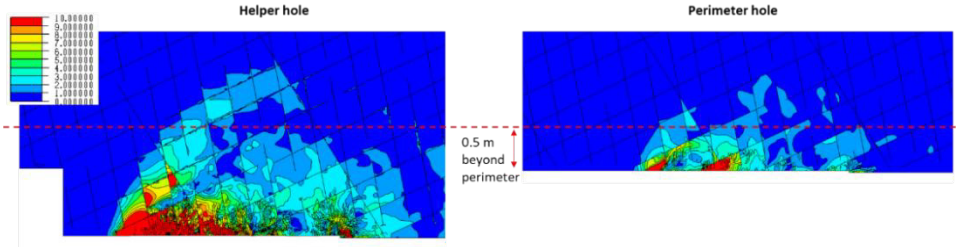


Figure 3. Simulation output for the siltstone/sandstone showing stress waves radiation off the helper (left) and perimeter (right) detonating charges with color contours of resultant velocity (0-10 m/s).

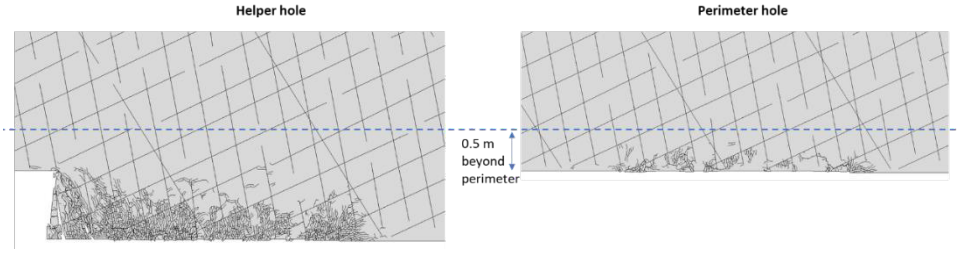


Figure 4. Simulation output for the siltstone/sandstone showing extent of fracturing in the rock mass due to the helper (left) and perimeter (right) charges.

## 5 COMPARSION OF DAMAGE DUE TO CAVERN PERIMIETER DESIGNS

The two principal perimeter design methodologies applied on the project are smooth wall blasting, which involves charging alternate holes with perimeter bulk product, and close-spaced line drilling of uncharged holes. Numerical modelling has been conducted to evaluate the variation in damage at the perimeter using these two techniques.

Figure 5 shows a typical smooth wall design including the location of the perimeter and easer holes, which are of principal interest due to their proximity to the wall when evaluating damage in the tunnel walls. The combination of charged and uncharged holes in the design requires the modelling of the interaction of multiple holes, therefore, a section of wall will be modelled, as shown within the black broken line. The same section of perimeter will be modelled for the line drilling design (Figure 5). All the holes in the model sections are 45 mm in diameter.

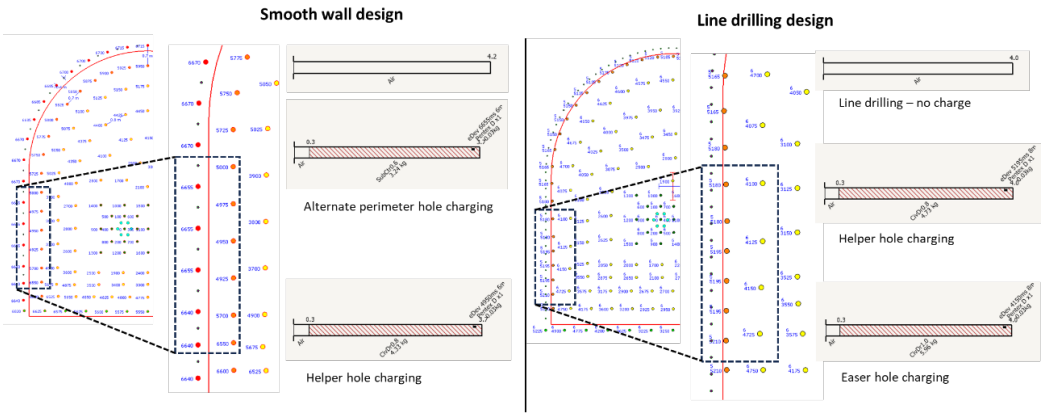


Figure 5. A typical smooth wall design (left), showing a close-up of the perimeter section modelled, and the charging of the perimeter (black and red) and helper holes (orange), and a line drilling design (right) showing a close-up of the wall section modelled, with the line holes (black) and the charging of the helper (orange) and easer holes (yellow).

While the rock mass elastic/plastic properties have remained the same between the two modelling studies, for the carven region the structural data has changed slightly (Table 3). Due to the scale of the perimeter hole designs, with hole spacings in the range 0.3 – 0.4 m, only the Bedding Plane and Joint Set 1 were built into the model geometry as discrete fracture networks. The nominal spacing of 2+ m for Joint Sets 2 and 3 would result in only one or two joints within the model.

Table 3. Rock mass discontinuity data - caverns.

| Structure | Bedding Plane | Joint Set 1 | Joint Set 2 | Joint Set 3 |
|---|---|---|---|---|
| Dip (°) | 30 | 79 | 81 | 84 |
| Dip Direction (°) | 058 | 122 | 053 | 276 |
| Nominal Spacing (m) | 0.3 | 0.3 | 2.0 | 2.0 |
| Nominal Persistence (m) | 5 | 2 | 5 | 5 |

### 5.1 *Cavern perimeter model geometries*

The cavern orientation and connecting tunnels are approximately northeast-southwest. Therefore, the plane of the model geometry is orientated northwest-southeast within the discontinuities (Table 3).

Figure 6 shows the plane strain model geometries for the two designs. The vertical extent of the model geometries is approximately 3.5 m, with 10 perimeter holes in the smooth wall geometry and 12 line holes in the line drilling design. The model geometry could not support the actual in-situ stresses of 19 MPa vertical and 29 MPa horizontal. Therefore, the models were run with stresses at 10 MPa vertical and 15 MPa horizontal. The reduced stresses will likely result in a marginal overestimation of the damage accumulated in the tunnel wall; however, the relative comparisons between the two designs should not be affected.

The line drilling model included easer and helper holes due to the proximity of the easer holes to the perimeter, and their potential to induce damage further from the holes because of the higher density bulk product (Figures 5 and 6). In contrast, the larger standoff of the easer holes in the smooth wall design would significantly reduce their potential to influence damage in the walls.

Simulations were run with the smooth wall and line drilling designs in the siltstone/sandstone and the more competent sandstone/siltstone.

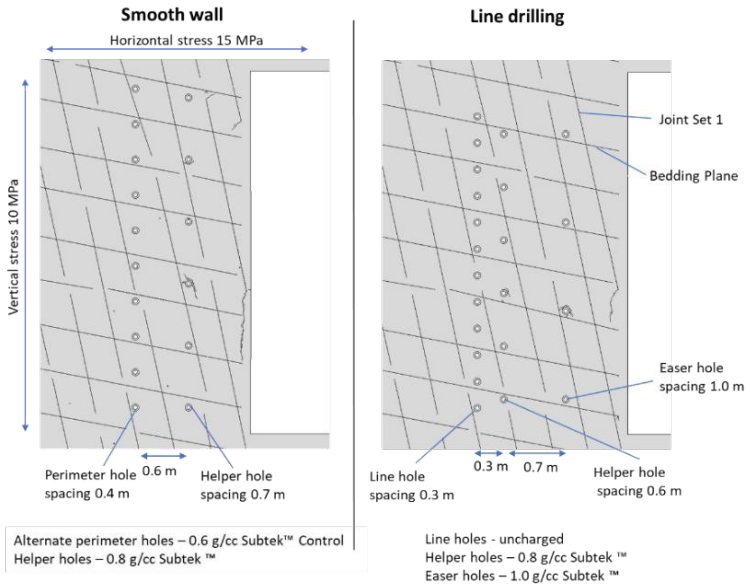


Figure 6. Model geometries for the smooth wall design (left) and the line drilling design (right).

## 5.2 *Cavern perimeter in siltstone/sandstone*

The simulation outputs for the smooth wall design (Figure 7a and 7b) show that after the helper holes have fired there is little fracturing beyond the perimeter holes. After the perimeter holes have fired, an effective fracture network forms between the holes to define the perimeter. However, there is a variation in the fracture network extending into the wall from the charged perimeter holes due to the influence of the Joint Set 1 structure. If the joint is close to the hole, the fractures are arrested by the joint. However, if the joint is further into the rock mass, fractures can extend further into the rock mass beyond the perimeter.

In the line drilling simulation, there is little damage accumulated at the perimeter after the easer holes have fired (Figure 7c). After the helper holes have fired, there is significant damage up to the location of the line holes (Figure 7d). However, there is not the same network of fractures between the line holes as is present in the smooth wall design (Figure 7b). This indicates that it could be harder to scale back to a clean wall with the line drilling, however, there is less damage in the rock mass at the perimeter with line drilling compared to the smooth wall design.

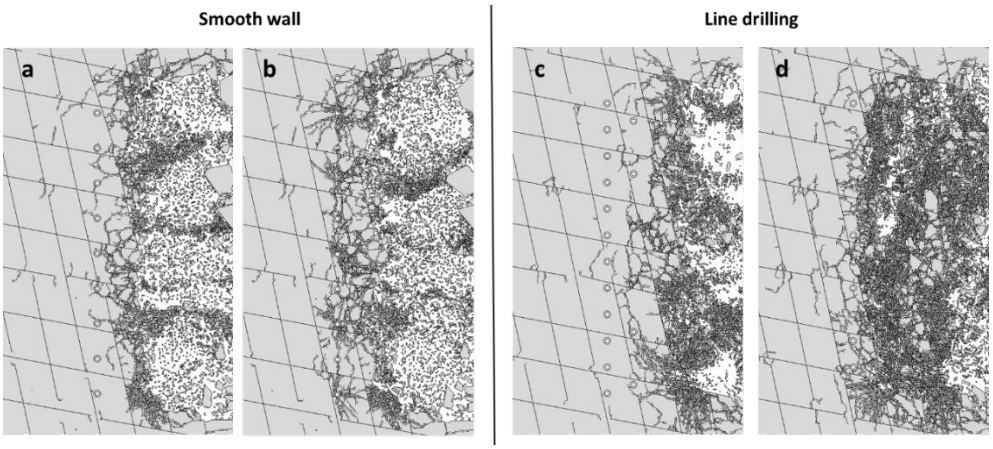


Figure 7. Smooth wall simulation after all the helper holes have fired (a) and after the perimeter holes have fired (b), and the line drilling simulation after all the easer holes have fired (c) and after the helper holes have fired (d) in siltstone/sandstone.

### 5.3 *Cavern perimeter in sandstone/siltstone*

The smooth wall design in the more competent sandstone/siltstone results in marginally more damage at the perimeter (Figure 8b) compared to the same design in the siltstone/sandstone (Figure 7b). This increase in damage in more competent rock is attributed to the higher strength rock sustaining higher stresses prior to failure, and subsequently undergoing more extensive fracturing as a result of the rock's sensitivity to strain rate. In contrast the line drilling simulation in the sandstone/siltstone (Figure 8d) has produced less damage in the perimeter compared to the same design in the siltstone/sandstone (Figure 7d). However, the overall trend comparing the damage due to the smooth wall design and the line drilling design is maintained across the two rock types.

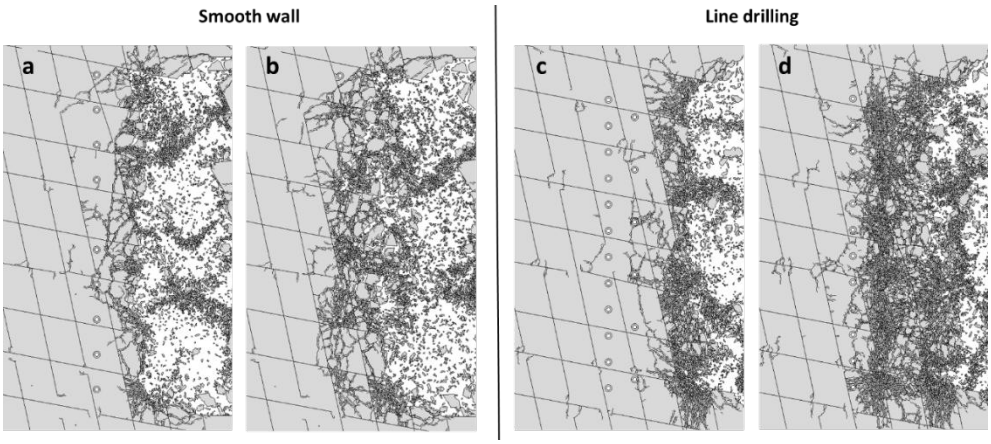


Figure 8. Smooth wall simulation after all the helper holes have fired (a) and after the perimeter holes have fired (b), and the line drilling simulation after all the easer holes have fired (c) and after the helper holes have fired (d) in sandstone/siltstone.

### 5.4 *Cavern modelling analysis*

The simulation outputs can be analysed to determine the length of new fractures created within a defined area. This enables a quantified assessment of the amount of damage that has been created within the models. Figure 9 shows how the rock mass behind the perimeter was divided into three regions to determine the damage created at the perimeter (0-0.1 m into the rock – blue region), further into the rock mass (0.1-0.2 m – green region), and then further still (0.2-0.5 m – orange region), across the four simulations. Table 4 lists the total new fractures created in the simulations for the three regions. The data shows that in the siltstone/sandstone the smooth wall design produces nearly twice as much damage at the perimeter (blue region) compared to the line drilling, however, further from the wall the amount of damage created is similar. In the sandstone/siltstone there is a larger difference between the damage due to smooth wall and line drilling designs, with the smooth wall design producing greater damage across all three regions.

Overall, the smooth wall design produces greater damage close to the perimeter, however, at distances greater than 0.2 m into the rock there is not a significant difference between the two designs in the amount of damage accumulated in the rock mass. The modelling also indicates that greater than 0.2 m into the perimeter the blast designs induce few new fractures into the rock mass.

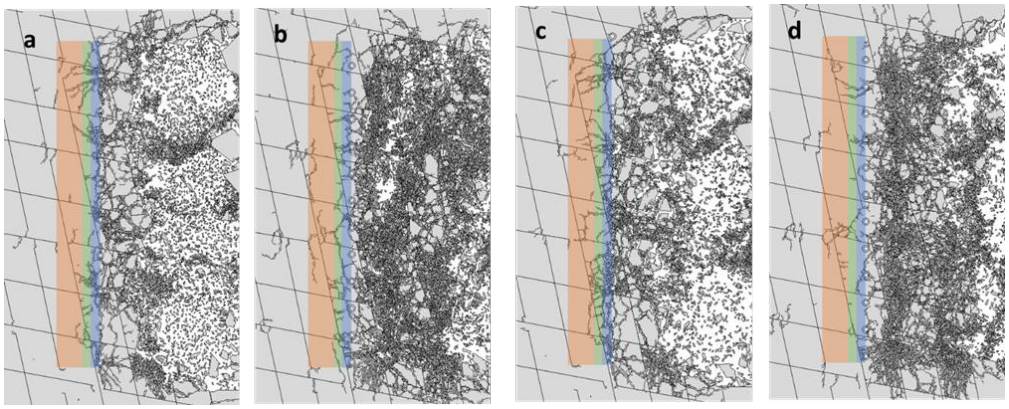

Figure 9. Simulation plots after all the holes have fired, showing the regions behind the wall analysed to calculate the total new fracture length created in the rock mass due to the blast for: siltstone/sandstone smooth wall (a), siltstone/sandstone line drilling (b), sandstone/siltstone smooth wall (c), and sandstone/siltstone line drilling (d).

Table 4. Total new fracture length at different regions away from the tunnel wall.

| Rock type | Perimeter design | Fracture length (m) for distances beyond the perimeter | | |
|---|---|---|---|---|
| | | 0-0.1 m | 0.1-0.2 m | 0.2-0.5 m |
| Siltstone/Sandstone | Smooth wall | 4.0 | 1.5 | 1.3 |
| Siltstone/Sandstone | Line drilling | 2.2 | 1.5 | 1.8 |
| Sandstone/Siltstone | Smooth wall | 5.8 | 1.9 | 2.2 |
| Sandstone/Siltstone | Line drilling | 1.5 | 0.7 | 1.4 |

## 6 CONCLUSIONS

High fidelity numerical modelling has been shown to be useful in determining the damage accumulating in the rock mass at the perimeter across a range of blast designs.

In the tunnel round, within the modelled rock mass and stress state, the helper holes have an appropriate standoff from the perimeter to minimize damage beyond the perimeter and the decoupled perimeter charge does not accumulate significant damage in the rock mass.

The comparison of two perimeter designs in the more critical cavern sections of the project highlights the smooth wall design, while requiring less drill meters, accumulates more damage at the perimeter than the line drill design. However, across the two rock types modelled neither design accumulates a significant amount of damage greater than 0.2 m beyond the perimeter.

## 7 REFERENCES

Backers, T. (2005): Fracture toughness determination and micromechanics of rock under mode I and mode II loading, PhD Thesis, (Scientific Technical Report STR ; 05/05), Potsdam : Deutsches GeoForschungsZentrum GFZ, 95 p.

Dare-Bryan, P.C., Mansfield, S. and Schoeman, S. (2012). Blast optimisation through computer modelling of fragmentation, heave and damage, *Proc. 10th International Symposium on Rock Fragmentation by Blasting*, New Delhi, India, 26-29 November, Rotterdam: Balkema, pp. 95-104.

Kirby, I., Chan, J. and Minchinton, A. (2014). Advances in predicting the effects of non-ideal detonation in blasting, in *Proc. 40th Annual Conference on Explosives and Blasting Techniques*, International Society of Explosives Engineers: Cleveland, pp. 301–314

Minchinton, A. and Lynch, P. M. (1996). Fragmentation and heave modelling using a coupled discrete element gas code, *Proc. 5th. Int. Symp. on Rock Fragmentation by Blasting*, Montreal, Canada, 25-29 Aug, A.A. Balkema, Rotterdam, pp. 71-80.

Owen, D.R.J., Munjiza, A. and Bicanic, N. (1992). A finite element-discrete element approach to the simulation of rock blasting problems, *Proc. 11th Symp. on finite elements in South Africa*, Centre for Research in Computational and Applied Mechanics, Cape Town, 15-17 Jan, pp. 39-58.